1 **Title: A single prophage WO gene rescues cytoplasmic incompatibility in *Drosophila melanogaster***

2

3 **Authors: J. Dylan Shropshire[1*], Jungmin On[1], Emily M. Layton[1], Helen Zhou[1], and Seth R.**

4 **Bordenstein[1,2,3,4*]**

5

6 [1]Department of Biological Sciences, Vanderbilt University, Nashville, TN 37235, USA

7 [2]Department of Pathology, Microbiology, and Immunology, Vanderbilt University, Nashville, TN 37235,

8 USA

9 [3]Vanderbilt Genetics Institute, Vanderbilt University, Nashville, TN 37235, USA

10 [4]Vanderbilt Institute of Infection, Immunology and Inflammation, Vanderbilt University, Nashville, TN

11 37235, USA

12 *Correspondence to:

13 J. Dylan Shropshire, Nashville, TN, 37235, Phone 423.930.6292, e-mail dylan.shropshire@vanderbilt.edu

14 Seth R. Bordenstein, Nashville, TN, 37235, Phone 615.322.9087, e-mail s.bordenstein@vanderbilt.edu

15

16 Mobile Title: *cifA* rescues cytoplasmic incompatibility

17

18 ORCID iD: J. Dylan Shropshire (https://orcid.org/0000-0003-4221-2178), Seth R. Bordenstein

19 (https://orcid.org/0000-0001-7346-0954)

20 Keywords: cytoplasmic incompatibility, rescue, *Wolbachia*, prophage WO, *Drosophila melanogaster*

21

Abstract: *Wolbachia* are maternally-inherited, intracellular bacteria at the forefront of vector control efforts to curb arbovirus transmission. In international field trials, the cytoplasmic incompatibility (CI) drive system of *w*Mel *Wolbachia* is deployed to replace target vector populations, whereby a *Wolbachia*–induced modification of the sperm genome kills embryos. However, *Wolbachia* in the embryo rescue the sperm genome impairment, and therefore CI results in a strong fitness advantage for infected females that transmit the bacteria to offspring. The two genes responsible for the *w*Mel-induced sperm modification of CI, *cifA* and *cifB*, were recently identified in the eukaryotic association module of prophage WO, but the genetic basis of rescue is unresolved. Here we use transgenic and cytological approaches to demonstrate that *cifA* independently rescues CI and nullifies embryonic death caused by *w*Mel *Wolbachia* in *Drosophila melanogaster*. Discovery of *cifA* as the rescue gene and previously one of two CI induction genes establishes a new 'Two-by-One' model that underpins the genetic basis of CI. Results highlight the central role of prophage WO in shaping *Wolbachia* phenotypes that are significant to arthropod evolution and vector control.

Significance Statement: The World Health Organization recommended pilot deployment of *Wolbachia*-infected mosquitoes to curb viral transmission to humans. Releases of mosquitoes are underway worldwide because *Wolbachia* can block replication of these pathogenic viruses and deterministically spread by a drive system termed cytoplasmic incompatibility (CI). Despite extensive research, the underlying genetic basis of CI remains only half-solved. We recently reported that two prophage WO genes recapitulate the modification component of CI in a released strain for vector control. Here we show that one of these genes underpins rescue of CI. Together, our results reveal the complete genetic basis of this selfish trait and pave the way for future studies exploring WO prophage genes as adjuncts or alternatives to current control efforts.

\body

Introduction:

Wolbachia are an archetype of maternally-inherited, intracellular bacteria. They occur in an estimated 40-52% of arthropod species (1, 2) and 47% of the Onchocercidae family of filarial nematodes (3), making them the most widespread bacterial symbiont in the animal kingdom (2). In arthropods, *Wolbachia* mainly reside in the cells of the reproductive tissues, transmit transovarially (4), and often commandeer host fertility, sex ratios, and sex determination to enhance their maternal transmission via male-killing, feminization, parthenogenesis, or cytoplasmic incompatibility (CI) (5, 6).

Discovered nearly half a century ago (7), *Wolbachia*-induced CI is the most common reproductive modification and results in embryonic lethality when an infected male mates with an uninfected female, but this lethality is rescued when the female is likewise infected (8). As such, rescue provides a strong fitness advantage to infected females, the transmitting sex of *Wolbachia* (9-11). Alone, CI-induced lethality is deployed in vector control studies to crash the resident uninfected mosquito population through release of *Wolbachia*-infected males (12-17). Together, CI-induced lethality and rescue constitute a microbial drive system that is used in field studies worldwide to stably replace an uninfected mosquito population with an infected one via release of male and females harboring *w*Mel *Wolbachia* (18), which confer resistance against dengue and Zika viruses (19, 20). The efficacy of this drive system for spreading *Wolbachia* in target populations critically depends on *Wolbachia's* ability to rescue its own lethal modification of the sperm.

While CI is gaining momentum as a natural, sustainable, and inexpensive tool for vector control, the genes that underpin this microbial adaptation are not fully known. Our previous screen of *Wolbachia* genomes and transcriptomes from infected ovaries identified two adjacent genes, *cifA* and *cifB*, from the *w*Mel strain in *Drosophila melanogaster* as the only genes consistently associated with CI (21). These two

genes occur in the eukaryotic association module of prophage WO (22), and they together recapitulate CI when dually expressed in uninfected male flies (21, 23). Each gene alone is incapable of inducing CI (21), and the rescue gene remains unknown. As *cifA* and *cifB* are the only two *w*Mel genes associated with CI, we previously hypothesized that the CI induction and rescue genes might be the same (21). Here we test the hypothesis that transgenic expression of *cifA* and/or *cifB* genes from *w*Mel *Wolbachia* in ovaries can rescue CI and nullify the associated embryonic defects in *D. melanogaster*.

Results and Discussion:

Since *Wolbachia* cannot be genetically transformed, we first tested the ability of *cifA* to transgenically rescue wild type CI using a GAL4-UAS system for tissue-specific expression in uninfected *D. melanogaster* females. As such, we conducted the transgenic experiments under the control of either *nos*-GAL4-*tubulin* in uninfected germline stem cells or maternal triple driver, MTD-GAL4, to drive higher transgene expression throughout oogenesis. In transcriptomes of *w*Mel-infected *D. melanogaster*, *cifA* is a highly expressed prophage WO gene (24). MTD-GAL4 utilizes two *nos*-GAL4 driver variants (including *nos*-GAL4-*tubulin*) and an ovarian tumor driver (25). Control CI and rescue crosses with either driver yielded the expected hatching rates. Crosses between infected males and uninfected females expressing *cifA* under the control of MTD-GAL4 showed a markedly significant increase in embryonic hatching relative to *cifA* expression under *nos*-GAL4-*tubulin* and at levels similar to that in control rescue crosses (Fig. 1A). These results are consistent with complete rescue of CI by *cifA*, in association with increased expression throughout the developing egg chambers. Similar results with *nos*-GAL4-*tubulin* expression in uninfected ovarian germline stem cells resulted in a small increase in hatch rate that was inconsistently significant among replicates (Fig. S1). An analysis of *cifA* gene expression reveals MTD-GAL4 associates with a three-

91 order-of-magnitude increase over *nos*-GAL4-*tubulin*, supporting strength of expression as a factor for
92 rescue (Fig. 1B).

93 We expanded our evaluation of *cif* gene expression under the control of MTD-GAL4 in uninfected
94 females to test if *cifB* alone or in combination with *cifA* impacts CI penetrance. As expected, infected
95 males crossed to either uninfected females or females transgenically expressing *cifB* under MTD-GAL4
96 yielded similar CI penetrance (Fig. 2). These results suggest that *cifB* does not rescue CI when
97 transgenically expressed in the ovaries, and its CI-related function is specific to testes. In contrast, MTD-
98 GAL4 expression of *cifA*, by itself or in combination with *cifB*, significantly rescued CI to levels comparable
99 to rescue by infected females (Fig. 2). These results are consistent with *cifA* independently functioning as
100 the rescue factor and suggest that *cifB* does not inhibit *cifA*'s ability to rescue CI. As *Wolbachia* can induce
101 phenotypes known to bias sex ratios, we collected the surviving offspring from the transgenic and control
102 rescue crosses and sexed them to demonstrate normal sex ratios, indicating that rescue was not sex-
103 specific (Fig. S2).

104 Next, we tested if the canonical cytological defects observed in early CI embryos (early mitotic
105 failure, chromatin bridging, and regional mitotic failure (26)) were nullified under *cifA*-induced rescue. We
106 examined embryos from control and transgenic crosses after 1-2 h of development and binned their
107 cytology into one of five phenotypes as previously established for *D. melanogaster* CI (21). Nearly half of
108 CI-induced lethality in embryos is the result of embryonic arrest during advanced developmental stages
109 in Dipteran species (27-30). As expected, the control CI cross yielded high levels of all three CI-associated
110 defects, and the embryos from the control rescue cross developed with significantly fewer abnormalities
111 (Fig. 3). MTD-GAL4 transgene expression of *cifA* in uninfected females, either alone or dually expressed
112 with *cifB*, resulted in significantly fewer cytological defects (Fig. 3). These effects were not seen with
113 transgene *cifB* expression, again validating that *cifA* alone can recapitulate wild type rescue by *Wolbachia*.

114 These data are in contrast with previous work reporting the inability to transgenically rescue CI in
115 *D. melanogaster (23)*; however, there are three critical differences between the studies. First, *w*Pip's
116 homologs from *Culex pipiens* were used in the prior work instead of *w*Mel's *cif* genes from *D.*
117 *melanogaster* here. Thus, differences in host background interactions could explain the discrepancy.
118 Second, a T2A sequence for the wPip gene homologs was used to allow for bicistronic expression, but
119 ribosome skipping results in a C-terminal sequence extension to the first protein and a proline addition to
120 the second protein that generates sequence artifacts and could alter function (31). Finally, different
121 insertion sites are capable of different levels of expression due to their local chromatin environment (32),
122 thus the chosen sites may produce insufficient product to cause rescue, as was the case in our study when
123 *cifA* was driven by *nos*-GAL4-*tubulin*.

124 *cifA* encodes a putative catalase-rel function, sterile-like transcription factor (STE) domains, and a
125 domain of unknown function (DUF3243) that shares homology with a putative Puf-family RNA binding
126 domain in *cifA*-like homologs (33), whereas *cifB* has nuclease and deubiquitilase domains (23, 33). Only
127 the deubiquitilase annotation has been functionally tested and confirmed(23). Based on subcellular
128 localization (PSORTb) and transmembrane helix predictors (TMbase), CifA is a cytoplasmic protein without
129 transmembrane helices (Fig. S3). Codon-based and Fisher's exact tests of neutrality demonstrate that
130 closely-related (76.2-99.8% pairwise nucleotide identity) Type I CifA homologs (21) largely evolve by
131 purifying selection (Fig. S4a, b), and sliding window analyses (SWAKK and JCoDA) reveal that purifying
132 selection is strongest on the catalase-rel domain and the unannotated region at the N-terminus, with
133 considerably weaker purifying selection on the putative DUF3243 and STE domains (Fig. 4; Fig. S4c). This
134 is supported by prior work reporting stronger amino acid conservation within the Type I CifA N-terminus
135 relative to the C-terminus (33).

136 These findings illustrate that the *Wolbachia* prophage WO gene *cifA* recapitulates rescue of wild
137 type CI. As *cifA* is one of two genes involved in induction of CI, results support the hypothesis that a gene

138 involved in CI induction is also the rescue gene (21). In addition, transgenic expression of *cifA* in yeast
139 inhibits a temperature-dependent growth defect caused by *cifB* expression (23). The discovery that CI is
140 induced by *cifA* and *cifB* and rescued by *cifA* motivates a new modification-rescue model of CI where two
141 genes act as the CI modification factors (in the male), and one of these same genes acts as the rescue
142 factor (in the female). This 'Two-by-One' model posits that each strain of *Wolbachia* has its own set of
143 *cifA*- and *cifB*-associated CI modifications and one *cifA* rescue factor. The different roles of *cifA* in CI and
144 rescue is intriguing. We predict that the function of *cifA* is dependent on differential tissue localization of
145 gene products in male and female reproductive systems and/or alternate post-translational modification
146 in testes/sperm (CI) versus in ovaries/embryoes (rescue). Moreover, one could speculate that the putative
147 antioxidant catalase-rel domain of the CifA protein acts as a functional switch in the presence of reactive
148 oxygen species, known to be higher in *Wolbachia*-infected testes (34), whereas the Puf-family RNA binding
149 domain and STE are involved in RNA binding and transcriptional (mis)regulation of an unknown host
150 factor.

151 It has been hypothesized that divergence in modification and rescue genes leads to bidirectional
152 CI (21, 37, 38), which is a reciprocal incompatibility between males and females infected with different
153 *Wolbachia* strains (7, 39-42). Comparative genomic analyses of *cifA* and *cifB* genes reveal extremely high
154 levels of amino acid divergence (21), strong codivergence (21, 33), and recombination (38), consistent
155 with the very rapid evolution of bidirectional CI across *Wolbachia* that can contribute to reproductive
156 isolation and speciation (42, 43). Indeed, divergence of the *cifA* and *cifB* genes into several phylogenetic
157 types correlates with bidirectional CI patterns in *Drosophila* and *Culex* (21, 38). There are at least two
158 explanations for how simple genetic changes in these genes can contribute to bidirectional CI. First, a
159 single mutation in the *cifA* gene could produce variation in the modification and rescue components that
160 render two *Wolbachia* strains incompatible. For instance, given an ancestral and derived allele of *cifA*,
161 males and females with *Wolbachia* carrying the same *cifA* allele are compatible; however, males with

162 *Wolbachia* carrying the ancestral *cifA* allele cause a sperm modification that is unable to be rescued by
163 embryos with *Wolbachia* carrying the derived *cifA* allele, and vice versa. Thus, a single mutation in *cifA*
164 alone can enable the switch from being compatible to incompatible *Wolbachia*. Second, mutations in both
165 *cifA* and *cifB* are required for the evolution of bidirectional CI. For example, CifA-CifB protein binding (23)
166 and/or differential localization in the sperm and egg may underpin bidirectional CI between *Wolbachia*
167 strains. In this model, amino acid divergence in the Cif proteins may contribute to weakened binding,
168 which in turn yields *Wolbachia* strains incapable of CI but capable of rescuing the ancestral variant (44,
169 45). A compensatory substitution in the other Cif protein could in theory restore binding and yield
170 bidirectional incompatibility with the ancestral Cif variants. Codivergence between amino acid sequences
171 of these proteins is consistent with this model. Under both models, the presence of multiple WO
172 prophages carrying *cifA* genes may also promote incompatibilities through the production of multiple CI
173 product complexes simultaneously (21). In support of these hypotheses, complex diversification and
174 duplication of *cifA* and *cifB* has been reported in *Drosophila* and *C. pipiens* that harbor a variety of
175 incompatible *Wolbachia* strains (21, 38).

176 In conclusion, our findings reveal the connected genetic basis of CI and rescue and highlight the
177 fundamental impact of prophage genes on the adaptive phenotypes of an obligate intracellular bacteria.
178 In addition to genetically dissecting this widespread form of reproductive parasitism and microbial drive,
179 we also establish a new, Two-by-One model to explain the modification and rescue components of CI.
180 Finally, beneficial applications of CI and rescue genes as transgenic drive constructs may be possible as
181 adjuncts or alternatives to pest control or vector control strategies currently deploying *Wolbachia*-
182 infected mosquitoes (15-18).

183

184

185 **Materials and Methods:**

186 ***Fly rearing and strains****. D. melanogaster* stocks y^1w^* (BDSC 1495), *nos*-GAL4-*tubulin* (BDSC 4442),
187 MTD-GAL4 (containing *nos*-GAL4-*tubulin*, nos-GAL4-VP16, and *otu*-GAL4-VP16; BDSC 31777), and UAS
188 transgenic lines homozygous for *cifA*, *cifB*, and *cifA;B* (21) were maintained at 12:12 light:dark at 25 ^{o} C
189 and 70% relative humidity (RH) on 50 ml of a standard media. GAL4 lines were found to be infected with
190 *w*Mel *Wolbachia*, and uninfected lines were produced through tetracycline treatment as previously
191 described (21). Infection status was frequently confirmed via PCR using WolbF and WolbR3 primers (46).
192 During virgin collections, flies were stored at 18 ^{o} C overnight to slow eclosion rate, and virgin flies were
193 kept at room temperature.

194 ***Hatch rate and sex ratio assays.*** Virgin MTD-GAL4 females were collected for the first 3 days of
195 emergence and aged 9-11 days before crossing to non-virgin homozygous UAS (*cifA*, *cifB*, or *cifA;B*) males.
196 The start of collections for the maternal and paternal lineages were staggered by 7 days. Single pair
197 matings occurred in an 8 oz bottle, and a grape-juice agar plate was smeared with yeast and affixed to the
198 opening with tape. The flies and bottles were then stored at 25 ^{o} C and 70% RH for 24 h at which time the
199 plates were replaced with freshly smeared plates and again stored for 24 h. Plates were then removed
200 and the number of embryos on each plate were counted and stored. After 30 h the remaining unhatched
201 embryos were counted (Extended Data Fig. 6). The hatch rate was calculated by dividing the number of
202 hatched embryos by the initial embryo count and multiplying by 100. Hatch rate was plotted against clutch
203 size for all rescue crosses conducted in this study to reveal a significant correlation (Fig. S5), and a
204 threshold clutch size for analysis was set equal to exclusion of 99% of plates with a hatch rate of 0 for each
205 genotype (31 for *nos*-GAL4-*tubulin* and 48 for MTD-GAL4). Larvae were moved into vials of standard media
206 and the offspring sex ratio determined after 15-18 days (Fig. S6). Hatch rates testing MTD-GAL4 or *nos*-
207 GAL4-*tubulin* expression of *cifA* were conducted three and four times respectively. Sex ratio experiments
208 were conducted once.

209 ***Gene expression.*** To compare the level of UAS-*cifA* expression between MTD-GAL4 and *nos*-GAL4-
210 *tubulin* flies, mothers from hatch rate assays were collected after the allotted laying period, abdomens
211 were immediately dissected, and samples were frozen in liquid nitrogen and stored at -80C until
212 processing. RNA was extracted using the Direct-zol RNA MiniPrep Kit (Zymo), DNase treated with DNA-
213 free (Ambion, Life Technologies), and cDNA was generated with SuperScript VILO (Invitrogen).
214 Quantitative PCR was performed on a Bio-Rad CFX-96 Real-Time System using iTaq Universal SYBR Green
215 Supermix (Bio-Rad). Forty cycles of PCR were performed against positive controls (extracted DNA),
216 negative controls (water), RNA, and cDNA with the following conditions: 50 °C 10 min, 95 °C 5 min, 40×
217 (95 °C 10 s, 55 °C 30 s), 95 °C 30 s. Primers used were *cifA* opt and Rp49 forward and reverse (Table S1).
218 Fold expression of UAS-*cifA* relative to the *D. melanogaster* house-keeping gene Rp49 was determined
219 with $2^{-\Delta\Delta Ct}$. This experiment and corresponding hatch rate were performed once.

220 ***Embryo cytology.*** Flies were collected as described for the hatch rate assays, but with 60 females
221 and 12 males in each bottle with a grape-juice agar plate attached. All flies used were siblings of those
222 from the hatch rate, grape-juice plates replaced as described above, and embryos collected in parallel to
223 egg-laying by hatch rate females. Embryos were collected, dechorionated, washed, methanol fixed,
224 stained with propidium iodide, imaged, and categorized as previously described (21) (Fig. S6). This
225 experiment was performed once.

226 ***Putative cifA localization.*** The PSORTb v3.0.2 web server (47) was used to predict subcellular
227 localization of the *w*Mel CifA protein to either the cytoplasm, cytoplasmic membrane, periplasm, outer
228 membrane, or extracellular space. A localization score is provided for each location with scores of 7.5 or
229 greater considered probable localizations. The TMpred web server (48) was used to predict
230 transmembrane helices in *w*Mel CifA. TMpred scores were generated for transmembrane helices
231 spanning from inside-to-outside (i-o) and outside-to-inside (o-i), and scores above 500 are considered
232 significant.

233 ***cifA selection analyses.*** Selection analyses were conducted using four independent tests of
234 selection: codon-based Z-test of neutrality (49), Fisher's exact test of neutrality (49), Sliding Window
235 Analysis of Ka and Ks (SWAKK) (50), and Java Codon Delimited Alignment (JCoDA) (51). The first two
236 analyses were conducted using the MEGA7 desktop app with a MUSCLE translation alignment generated
237 in Geneious v5.5.9. The SWAKK 2.1 web server and the JCoDA v1.4 desktop app were used to analyze
238 divergence between *w*Mel and *w*Ha *cifA* with a sliding window of 25 or 50 codons and a jump size of 1
239 codon for SWAKK and 5 codons for JCoDA.

240 ***Statistical analyses.*** All statistical analyses were conducted in GraphPad Prism (Prism 7 or online
241 tools). Hatch rate and sex ratio statistical comparisons were made using Kruskal-Wallis followed by a
242 Dunn's multiple comparison test. Expression was compared using a Mann-Whitney test. Correlations
243 between hatch rate and clutch size were determined using Spearman rho. Pair-wise chi-square analyses
244 were used for cytology studies to compare defective and normal embryos followed by generation of
245 Bonferroni adjusted p-values. An unpaired t-test was used for statistical comparison of RNA fold
246 expression. All p-values are reported in Table S2.

247 ***Data availability.*** All source data and replicate data are available as Supplementary Information
248 along with this publication.

249

250

Acknowledgments: This work was supported by National Institutes of Health (NIH) awards R01 AI132581 and R21 HD086833 to S.R.B., National Science Foundation award IOS 1456778 to S.R.B., and a National Science Foundation Graduate Research Fellowship to J.D.S. Any opinion, findings, and conclusions or recommendations expressed in this material are those of the authors(s) and do not necessarily reflect the views of the National Institutes of Health or the National Science Foundation. Imaging was performed in part using the Vanderbilt University Medical Center Cell Imaging Shared Resources (supported by NIH grants CA68485, DK20593, DK58404, DK59637 and EY08126). We thank Daniel LePage for preliminary work, Sarah R. Bordenstein and Jessamyn Perlmutter for manuscript preparation, and Jared Nordman for kindly providing the MTD-GAL4 line.

262 **References:**

263 1. Weinert LA, Araujo-Jnr EV, Ahmed MZ, & Welch JJ (2015) The incidence of bacterial
264 endosymbionts in terrestrial arthropods. *Proc Biol Sci* 282(1807):20150249.
265 2. Zug R & Hammerstein P (2012) Still a host of hosts for *Wolbachia*: analysis of recent data
266 suggests that 40% of terrestrial arthropod species are infected. *PLoS One* 7(6):e38544.
267 3. Ferri E*, et al.* (2011) New insights into the evolution of *Wolbachia* infections in filarial nematodes
268 inferred from a large range of screened species. *PLoS One* 6(6):e20843.
269 4. Frydman HM, Li JM, Robson DN, & Wieschaus E (2006) Somatic stem cell niche tropism in
270 *Wolbachia*. *Nature* 441(7092):509-512.
271 5. Werren JH, Baldo L, & Clark ME (2008) *Wolbachia*: master manipulators of invertebrate biology.
272 *Nat Rev Microbiol* 6(10):741-751.
273 6. LePage D & Bordenstein SR (2013) *Wolbachia*: Can we save lives with a great pandemic? *Trends*
274 *in parasitology* 29(8):385-393.
275 7. Yen J & Barb A (1973) The etiological agent of cytoplasmic incompatability in *Culex pipiens*.
276 *Journal of Invertebrate Pathology* 22.
277 8. Serbus LR, Casper-Lindley C, Landmann F, & Sullivan W (2008) The genetics and cell biology of
278 *Wolbachia*-host interactions. *Annu Rev Genet* 42:683-707.
279 9. Turelli M & Hoffmann AA (1999) Microbe-induced cytoplasmic incompatibility as a mechanism
280 for introducing transgenes into arthropod populations. *Insect Mol Biol* 8(2):243-255.
281 10. Hancock PA, Sinkins SP, & Godfray HC (2011) Strategies for introducing *Wolbachia* to reduce
282 transmission of mosquito-borne diseases. *PLoS Negl Trop Dis* 5(4):e1024.
283 11. Hancock PA, Sinkins SP, & Godfray HC (2011) Population dynamic models of the spread of
284 *Wolbachia*. *Am Nat* 177(3):323-333.
285 12. Atyame CM*, et al.* (2011) Cytoplasmic incompatibility as a means of controlling *Culex pipiens*
286 quinquefasciatus mosquito in the islands of the south-western Indian Ocean. *PLoS Negl Trop Dis*
287 5(12):e1440.
288 13. Dobson SL, Bordenstein SR, & Rose RI (2016) *Wolbachia* mosquito control: Regulated. *Science*
289 352(6285):526-527.
290 14. O'Connor L*, et al.* (2012) Open release of male mosquitoes infected with a *Wolbachia*
291 biopesticide: field performance and infection containment. *PLoS Negl Trop Dis* 6(11):e1797.
292 15. Zhang D, Zheng X, Xi Z, Bourtzis K, & Gilles JR (2015) Combining the sterile insect technique with
293 the incompatible insect technique: I-impact of *Wolbachia* infection on the fitness of triple- and
294 double-infected strains of *Aedes albopictus*. *PLoS One* 10(4):e0121126.
295 16. Ritchie SA, Townsend M, Paton CJ, Callahan AG, & Hoffmann AA (2015) Application of *w*MelPop
296 *Wolbachia* strain to crash local populations of *Aedes aegypti*. *PLoS Negl Trop Dis* 9(7):e0003930.
297 17. Zabalou S*, et al.* (2004) *Wolbachia*-induced cytoplasmic incompatibility as a means for insect
298 pest population control. *Proc Natl Acad Sci U S A* 101(42):15042-15045.
299 18. Hoffmann AA*, et al.* (2014) Stability of the *w*Mel *Wolbachia* infection following invasion into
300 *Aedes aegypti* populations. *PLoS Negl Trop Dis* 8(9):e3115.
301 19. Walker T*, et al.* (2011) The *w*Mel *Wolbachia* strain blocks dengue and invades caged *Aedes*
302 *aegypti* populations. *Nature* 476(7361):450-453.
303 20. Dutra HL*, et al.* (2016) *Wolbachia* blocks currently circulating Zika virus isolates in Brazilian
304 *Aedes aegypti* mosquitoes. *Cell Host Microbe* 19(6):771-774.
305 21. LePage DP*, et al.* (2017) Prophage WO genes recapitulate and enhance *Wolbachia*-induced
306 cytoplasmic incompatibility. *Nature* 543(7644):243-247.

307 22. Bordenstein SR & Bordenstein SR (2016) Eukaryotic association module in phage WO genomes
308 from *Wolbachia*. *Nat Commun* 7:13155.
309 23. Beckmann JF, Ronau JA, & Hochstrasser M (2017) A *Wolbachia* deubiquitylating enzyme induces
310 cytoplasmic incompatibility. *Nat Microbiol* 2:17007.
311 24. Gutzwiller F*, et al.* (2015) Dynamics of *Wolbachia* pipientis Gene Expression Across the
312 *Drosophila melanogaster* Life Cycle. *G3 (Bethesda)* 5(12):2843-2856.
313 25. Staller MV*, et al.* (2013) Depleting gene activities in early *Drosophila* embryos with the
314 "maternal-Gal4-shRNA" system. *Genetics* 193(1):51-61.
315 26. Landmann F, Orsi GA, Loppin B, & Sullivan W (2009) *Wolbachia*-mediated cytoplasmic
316 incompatibility is associated with impaired histone deposition in the male pronucleus. *PLoS*
317 *Pathog* 5(3):e1000343.
318 27. Lassy CW & Karr TL (1996) Cytological analysis of fertilization and early embryonic development
319 in incompatible crosses of *Drosophila simulans*. *Mechanisms of development* 57(1):47-58.
320 28. Callaini G, Riparbelli MG, Giordano R, & Dallai R (1996) Mitotic defects associated with
321 cytoplasmic incompatibility in *Drosophila simulans*. *Journal of Invertebrate Pathology* 67(1):55-
322 64.
323 29. Wright JD & Barr AR (1981) *Wolbachia* and the normal and incompatible eggs of *Aedes*
324 *polynesiensis* (Diptera: Culicidae). *Journal of Invertebrate Pathology* 38(3):409-418.
325 30. Duron O & Weill M (2006) *Wolbachia* infection influences the development of *Culex pipiens*
326 embryo in incompatible crosses. *Heredity (Edinb)* 96(6):493-500.
327 31. Donnelly ML*, et al.* (2001) Analysis of the aphthovirus 2A/2B polyprotein 'cleavage' mechanism
328 indicates not a proteolytic reaction, but a novel translational effect: a putative ribosomal 'skip'.
329 *The Journal of general virology* 82(Pt 5):1013-1025.
330 32. Akhtar W*, et al.* (2013) Chromatin Position Effects Assayed by Thousands of Reporters
331 Integrated in Parallel. *Cell* 154(4):914-927.
332 33. Lindsey ARI*, et al.* (2018) Evolutionary genetics of cytoplasmic incompatibility genes *cifA* and *cifB*
333 in prophage WO of *Wolbachia*. *Genome biology and evolution* 10(2):435-451.
334 34. Brennan LJ, Haukedal JA, Earle JC, Keddie B, & Harris HL (2012) Disruption of redox homeostasis
335 leads to oxidative DNA damage in spermatocytes of Wolbachia-infected Drosophila simulans.
336 *Insect Mol Biol* 21(5):510-520.
337 35. Penz T*, et al.* (2012) Comparative genomics suggests an independent origin of cytoplasmic
338 incompatibility in *Cardinium hertigii*. *PLoS Genet* 8(10):e1003012.
339 36. Mann E*, et al.* (2017) Transcriptome Sequencing Reveals Novel Candidate Genes for *Cardinium*
340 *hertigii*-Caused Cytoplasmic Incompatibility and Host-Cell Interaction. *mSystems* 2(6).
341 37. Charlat S, Calmet C, & Mercot H (2001) On the mod resc model and the evolution of Wolbachia
342 compatibility types. *Genetics* 159(4):1415-1422.
343 38. Bonneau M*, et al.* (2018) Culex pipiens crossing type diversity is governed by an amplified and
344 polymorphic operon of Wolbachia. *Nature Communications* 9(1):319.
345 39. O'Neill SL & Karr TL (1990) bidirectional incompatability between conspecific populations of
346 drosophila simulans. *Nature* 348:178-180.
347 40. Bordenstein SR & Werren JH (2007) Bidirectional incompatibility among divergent *Wolbachia*
348 and incompatibility level differences among closely related *Wolbachia* in *Nasonia*. *Heredity*
349 99(3):278-287.
350 41. Poinsot D, Bourtzis K, Markakis G, Savakis C, & Mercot H (1998) *Wolbachia* transfer from
351 *Drosophila melanogaster* into *D. simulans*: Host effect and cytoplasmic incompatibility
352 relationships. *Genetics* 150(1):227-237.
353 42. Bordenstein SR, O'Hara FP, & Werren JH (2001) *Wolbachia*-induced incompatibility precedes
354 other hybrid incompatibilities in *Nasonia*. *Nature* 409(6821):707-710.

355 43. Brucker RM & Bordenstein SR (2012) Speciation by symbiosis. *Trends in ecology & evolution*
356 27(8):443-451.
357 44. Zabalou S*, et al.* (2004) Natural *Wolbachia* infections in the *Drosophila yakuba* species complex
358 do not induce cytoplasmic incompatibility but fully rescue the *w*Ri modification. *Genetics*
359 167(2):827-834.
360 45. Bourtzis K, Dobson SL, Braig HR, & O'Neill SL (1998) Rescuing *Wolbachia* have been overlooked.
361 *Nature* 391(6670):852-853.
362 46. Casiraghi M, Anderson TJ, Bandi C, Bazzocchi C, & Genchi C (2001) A phylogenetic analysis of
363 filarial nematodes: comparison with the phylogeny of *Wolbachia* endosymbionts. *Parasitology*
364 122 Pt 1:93-103.
365 47. Yu NY*, et al.* (2010) PSORTb 3.0: improved protein subcellular localization prediction with
366 refined localization subcategories and predictive capabilities for all prokaryotes. *Bioinformatics*
367 *(Oxford, England)* 26(13):1608-1615.
368 48. Hofmann K (1993) TMbase-A database of membrane spanning proteins segments. *Biol. Chem.*
369 *Hoppe-Seyler* 374:166.
370 49. Kumar S, Stecher G, & Tamura K (2016) MEGA7: Molecular Evolutionary Genetics Analysis
371 Version 7.0 for Bigger Datasets. *Molecular biology and evolution* 33(7):1870-1874.
372 50. Liang H, Zhou W, & Landweber LF (2006) SWAKK: a web server for detecting positive selection in
373 proteins using a sliding window substitution rate analysis. *Nucleic Acids Res* 34(Web Server
374 issue):W382-384.
375 51. Steinway SN, Dannenfelser R, Laucius CD, Hayes JE, & Nayak S (2010) JCoDA: a tool for detecting
376 evolutionary selection. *BMC Bioinformatics* 11:284.

377

378

379 **Figure Legends:**

380 **Fig. 1. *cifA* rescues cytoplasmic incompatibility when it is highly expressed throughout oogenesis. (A)**
381 Hatch rate assays were conducted with transgenic expression of *cifA* under the control of *nos*-GAL4-
382 *tubulin* (germline stem cells) or MTD-GAL4 (oogenesis) drivers. Each dot represents a replicate. Rescue
383 occurred only under MTD-GAL4 expression. Horizontal dotted lines from top to bottom separate cross
384 types with CI, *cifA* expression, and rescue. *Wolbachia* infections are represented by filled sex symbols and
385 expressed genes are noted to the right of the corresponding sex. n=27-59 for each experimental cross
386 across two experiments (both shown). Vertical bars represent medians, and letters to the right indicate
387 significant differences based on α=0.05 calculated by Kruskal-Wallis and Dunn's test for multiple
388 comparisons. (B) Expression fold change of *cifA* relative to the *Drosophila* housekeeping gene Rp49 was
389 determined on a subset of abdomens from female expressing *cifA* via MTD-GAL4 or *nos*-GAL4-*tubulin* with
390 $2^{-\Delta\Delta Ct}$. Horizontal bars represent medians with 95% confidence intervals, and letters above indicate
391 significance based on a Mann-Whitney test. In both cases, statistical comparisons are between all groups.
392 Exact p-values are provided in Table S2. Hatch rate experiments testing expression of *cifA* under MTD-
393 GAL4 or *nos*-GAL4-*tubulin* have been repeated four and five times respectively.

394 **Fig. 2. Rescue of cytoplasmic incompatibility is specific to *cifA*.** Hatch rate assays were conducted with
395 transgenic expression of *cifA*, *cifB*, and *cifA;B* using the MTD-GAL4 driver for expression throughout
396 oogenesis. Each dot represents a replicate. *Wolbachia* infections are represented by filled sex symbols
397 and expressed genes are noted to the right of the corresponding sex. n=11-29 for each experimental cross.
398 Vertical bars represent medians, and letters to the right indicate significant differences based on α=0.05
399 calculated by Kruskal-Wallis and Dunn's test for multiple comparisons. Statistical comparisons are
400 between all groups. Exact p-values are provided in Table S2. Hatch rate experiments testing expression of
401 *cifA* under MTD-GAL4 have been repeated three times.

402 **Fig. 3. *cifA* rescues embryonic defects caused by cytoplasmic incompatibility.** The number of embryos
403 with each cytological phenotype resulting from the indicated crosses is shown. All replicate crosses were
404 conducted in parallel and with sisters from the experiment in Fig 2. *cifA*, *cifB*, and *cifA;B* transgene
405 expression was under the control of MTD-GAL4. *Wolbachia* infections are represented by filled sex
406 symbols and expressed genes are noted to the right of the corresponding sex. Letters to the right indicate
407 significant differences based on α=0.05 calculated by pair-wise chi-square analyses comparing defects (all
408 shades of red) against normal (blue) with Bonferroni adjusted p-values. Exact p-values are provided in
409 Table S2. This experiment has been conducted once.

410 **Fig. 4. Ka/Ks sliding window analysis identifies *cifA* regions evolving under negative selection.** A sliding
411 window analysis of Ka/Ks ratios between *cifA* homologs from *w*Mel and *w*Ha rejects the neutral
412 expectation of Ka/Ks = 1 using a 25 amino acid sliding window across most of *cifA*. (a) Strong purifying
413 selection is observed in several *cifA* regions including the sequence preceding the Catalase-rel domain.
414 Shaded regions denote previously described protein domain predictions (33).

415

Fig. S1. *cifA* transgene expression in germline stem cells fails to elicit rescue. Transgene expression of *cifA*, *cifB*, and *cifA;B* using the *nos*-GAL4-*tubulin* driver does not lead to rescue of cytoplasmic incompatibility. Each dot represents a replicate. *Wolbachia* infections are represented by filled sex symbols, and expressed genes are noted to the right of the corresponding sex. n=15-34 for each experimental cross. Vertical bars represent medians and letters to the right indicate significant differences based on α=0.05 calculated by Kruskal-Wallis and Dunn's test for multiple comparisons. Statistical comparisons are between all groups. Exact p-values are provided in Table S2.

Fig. S2. *cifA* does not preferentially rescue one sex over the other. Surviving offspring from the experiment displayed in Figure 2 were collected for adult sex ratio counts. There was no significant difference between any of the crosses. A sex ratio count was not possible for CI crosses due to the low number of surviving offspring. *Wolbachia* infections are represented by filled sex symbols and expressed genes are noted to the right of the corresponding sex. n=11-22 for each experimental cross. Vertical bars represent medians and letters to the right indicate significant differences based on α=0.05 calculated by Kruskal-Wallis and Dunn's test for multiple comparisons. Statistical comparisons are between all groups. Exact p-values are provided in Table S2. This experiment was conducted once.

Fig. S3. CifA is a putative cytoplasmic protein. (**A**) The PSORTb subcellular protein localization web server was used on Type I CifA proteins to predict the protein's localization in the *Wolbachia* cell. Predictive scores above 7.5 are accepted to be sufficient to determine a single location of localization and suggest that CifA is a cytoplasmic protein. (**B**) The TMpred web server was used to predict transmembrane helices. TMpred scores exceeding 500 (denoted by horizontal dotted line) are considered significant. TMpred scores were generated for transmembrane helices spanning from inside-to-outside (i-o) and outside-to-inside (o-i). Shaded regions denote previously described protein domain predictions (33).

Fig. S4. *cifA* regions evolve under negative selection. (**A**) Pairwise codon-based z-tests of selection suggest that regions of the *cifA* gene are not evolving under the neutral expectation of K_a=K_s. Values below

25 the diagonal are p-values for where there is a significant departure from neutrality or not. Values above
26 the diagonal are the difference of K_a-K_s in which positive values suggest positive selection and negative
27 values suggest purifying selection. (**B**) Pairwise Fisher's exact tests of neutrality suggest that *cifA* evolves
28 under purifying selection. Values below the diagonal are p-values. If the p-value is less than 0.05, then the
29 null hypothesis of strictly neutral or purifying selection is rejected. If the observed number
30 of synonymous differences per synonymous site exceeds the number of nonsynonymous differences per
31 nonsynonymous site then *MEGA* sets *P* = 1 to indicate purifying selection, rather than positive selection.
32 (**C**) SWAKK and JCoDA were used for sliding window analyses of Ka/Ks ratios between *cifA* homologs of
33 *w*Mel and the bidirectionally incompatible *w*Ha. Both programs were performed with 25 amino acid
34 windows and yield Ka/Ks ratios evident of strong purifying selection in the N-terminus region preceding
35 the Catalase-rel domain and weaker purifying selection beyond it. Shaded regions denote previously
36 described domain predictions (33).

37 **Fig. S5. Fertility is related to strain genotype.** A meta-analysis of all control rescue crosses (infected male
38 x infected female) without a transgene shows that clutch size and hatch rate are significantly correlated
39 for both the MTD-GAL4 and *nos*-GAL4-*tubulin* genotypes (r = 0.59 and 0.50 for MTD-GAL4 and *nos*-GAL4-
40 *tubulin* respectively), but the two strains have different y-intercepts (4.69 to 31.43 and 39.94 to 59.04 for
41 MTD-GAL4 and *nos*-GAL4-*tubulin* respectively). Each dot represents a replicate where circles and
42 diamonds are MTD-GAL4 (n=91) and *nos*-Gal4-*tubulin* (n=134) respectively. Vertical dotted lines represent
43 embryo counts where 99% of clutch sizes with 0% embryo hatch rate are to the left for *nos*-GAL4-*tubulin*
44 (left line) and MTD-GAL4 (right line). Correlation was assessed with Spearman Rho. A linear regression
45 best-fit line is plotted for each genotype. Exact p-values are provided in Table S2.

46 **Fig. S6. Schematic of experimental methodology.** (a) All experimental setups begin with the generation
47 of the maternal lineage (pink), derived from GAL4 driver lines and collected as virgins and aged for 6-8
48 days till the peak of their fecundity. (b) The paternal lineage (blue) is setup in a stagger such that the males

49 used in the experiment emerge on the day of the experiment. (c) Flies are crossed in a fashion dependent
50 on the ultimate intent, and grape-juice agar plates provided and replaced in a similar manner for all
51 experiments. Sex ratio studies are derived from hatch rate assays.

52

53

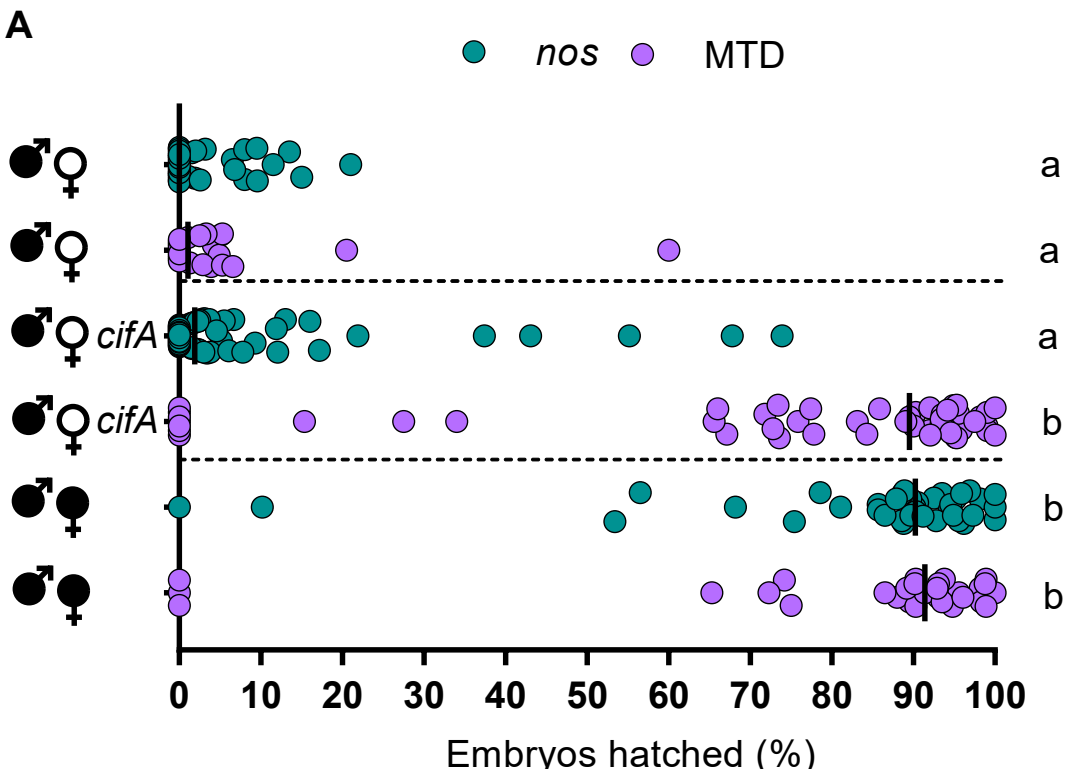
A
nos
MTD
cifA
cifA
a
a
a
b
b
b
0
10
20
30
40
50
60
70
80
90
100
Embryos hatched (%)

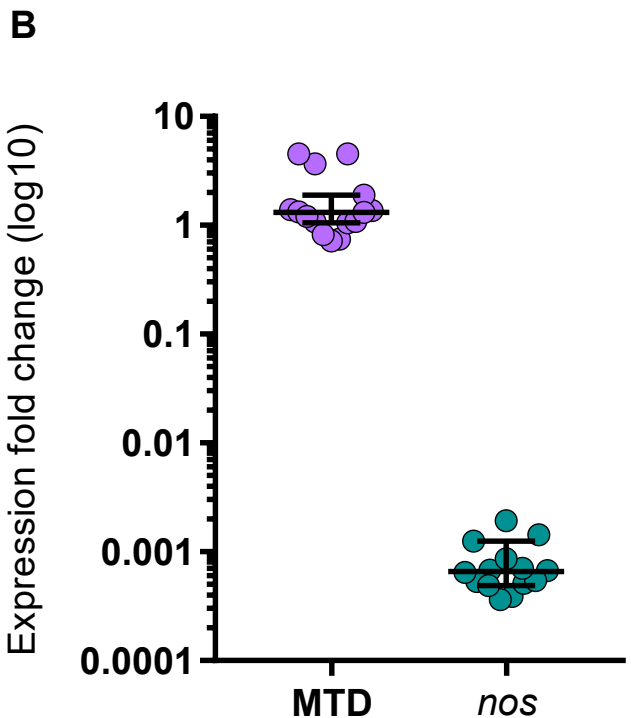
B
Expression fold change (log10)
10
1
0.1
0.01
0.001
0.0001
MTD
nos

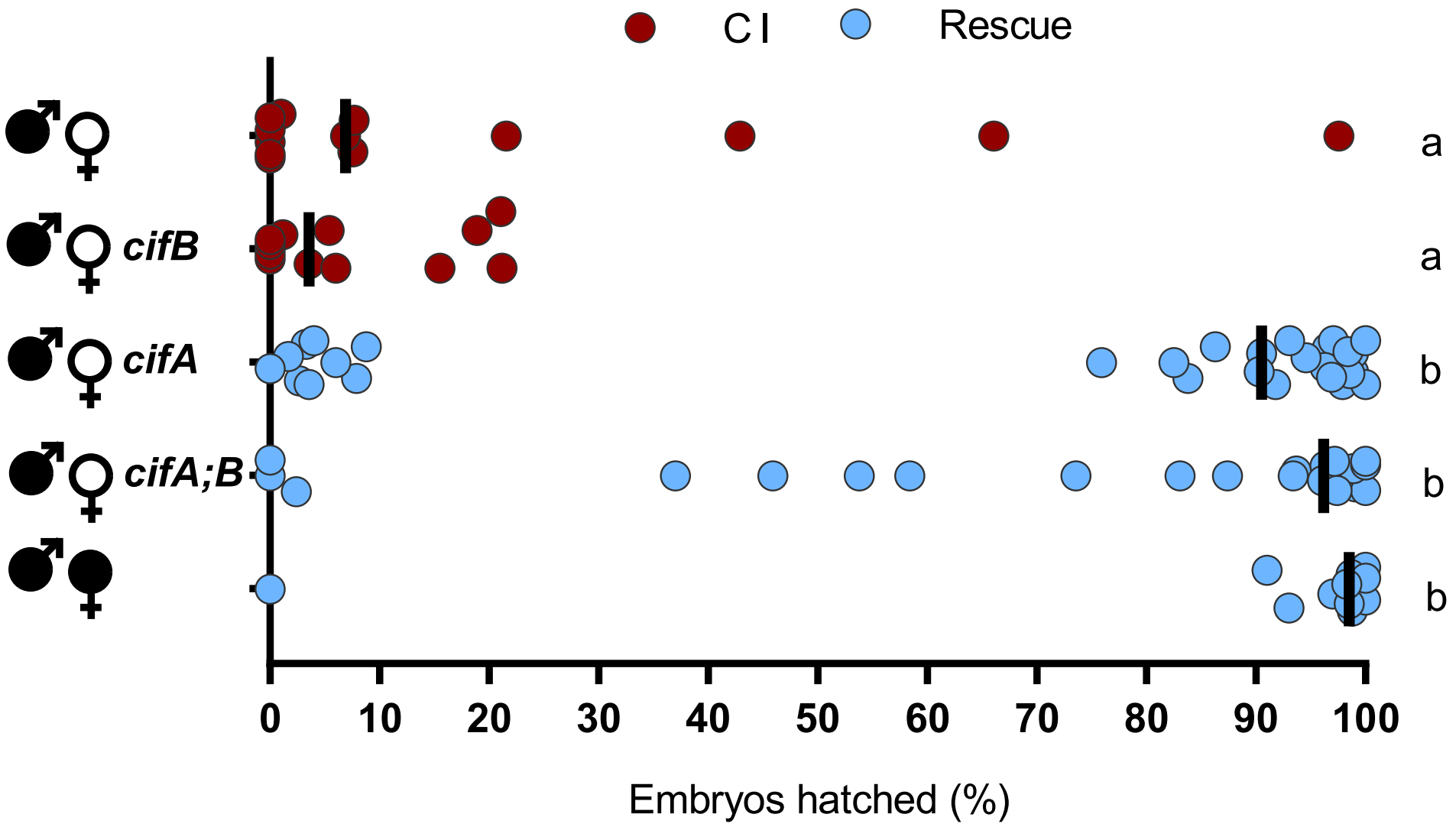
CI
Rescue
cifB
cifA
cifA;B
a
a
b
b
b
0
10
20
30
40
50
60
70
80
90
100
Embryos hatched (%)

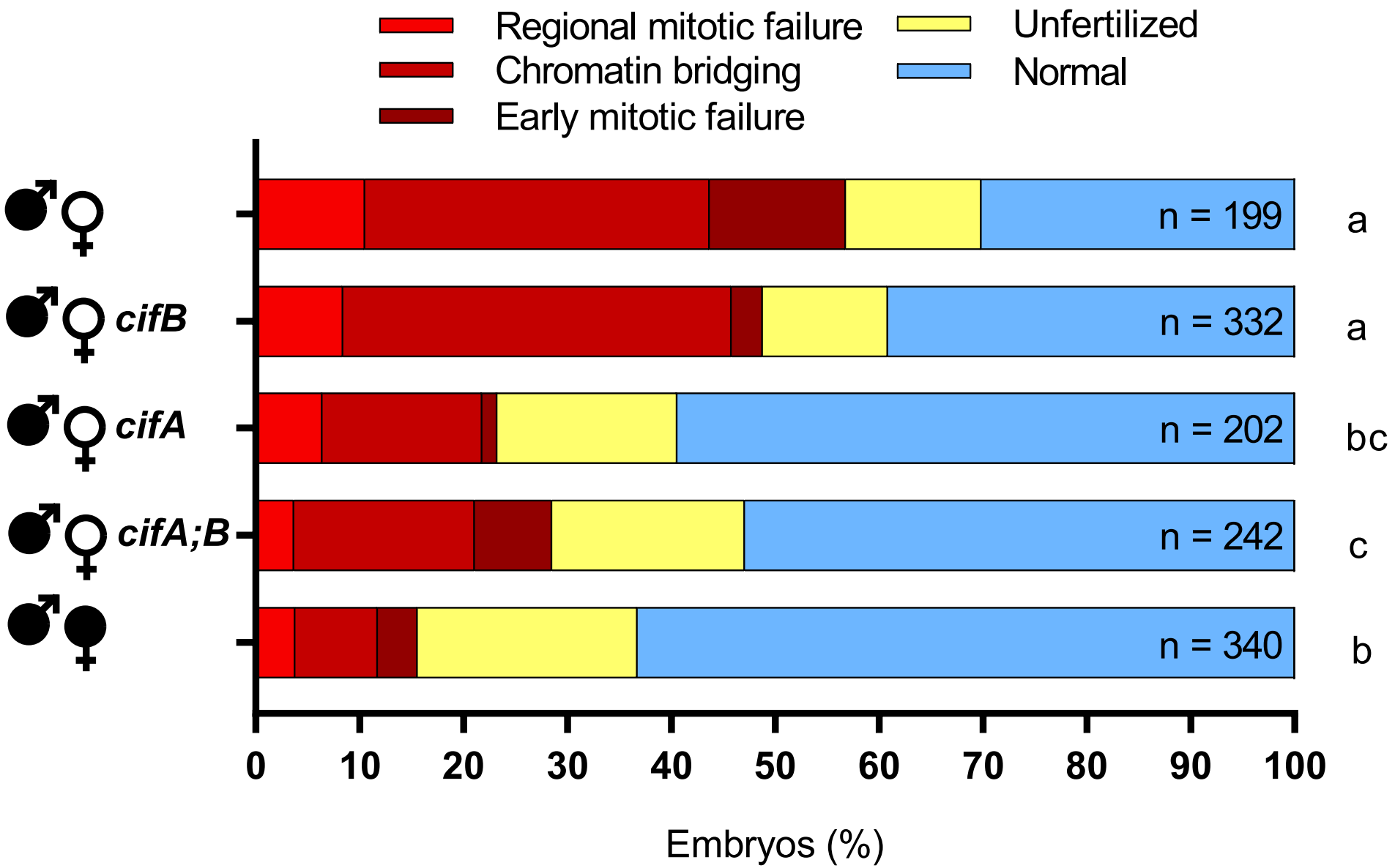
Regional mitotic failure
Chromatin bridging
Early mitotic failure
Unfertilized
Normal
♂♀
♂♀ cifB
♂♀ cifA
♂♀ cifA;B
♂♀
n = 199
n = 332
n = 202
n = 242
n = 340
a
a
bc
c
b
0
10
20
30
40
50
60
70
80
90
100
Embryos (%)

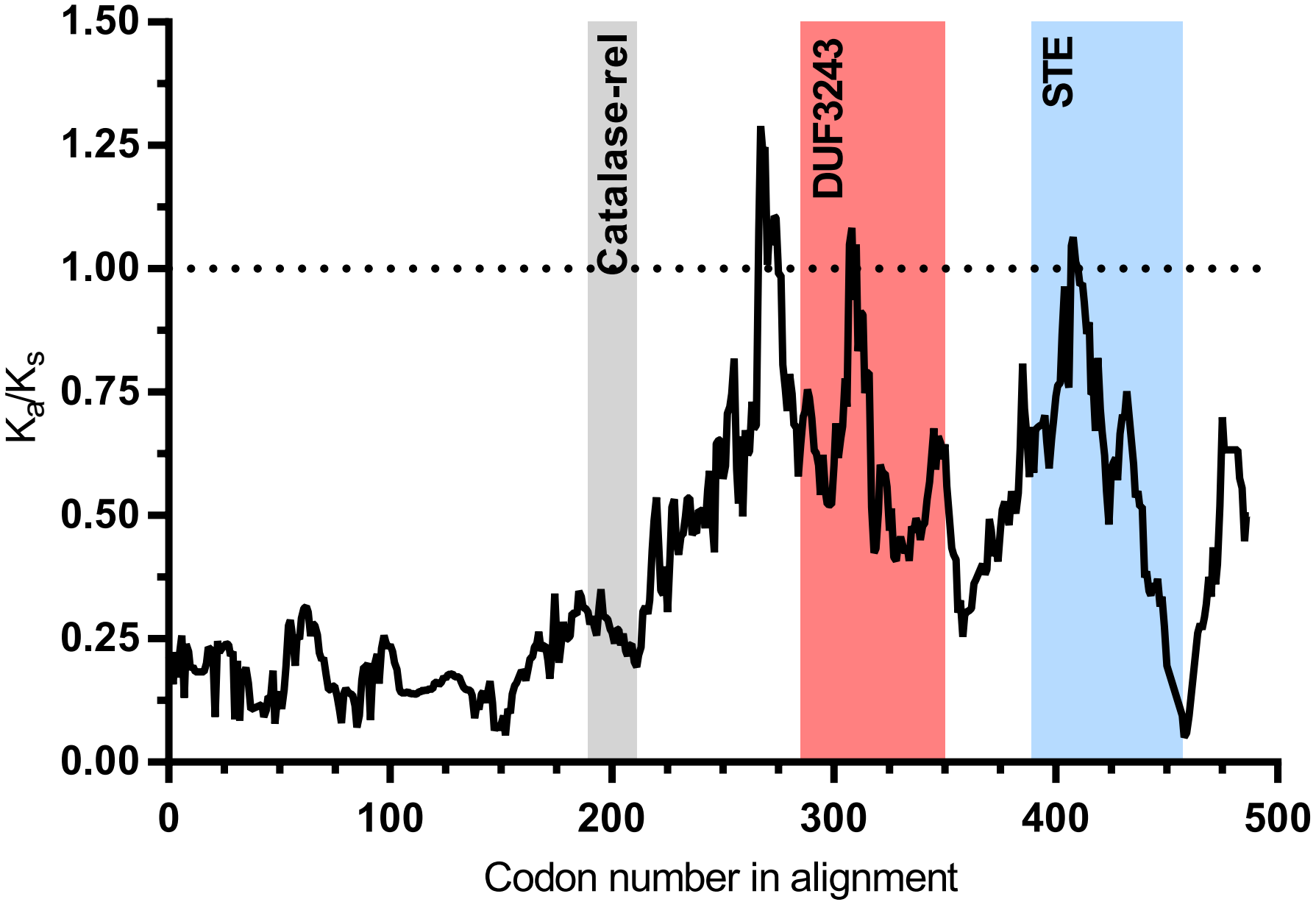
1.50
1.25
1.00
0.75
0.50
0.25
0.00
K_a/K_s
Catalase-rel
DUF3243
STE
0
100
200
300
400
500
Codon number in alignment

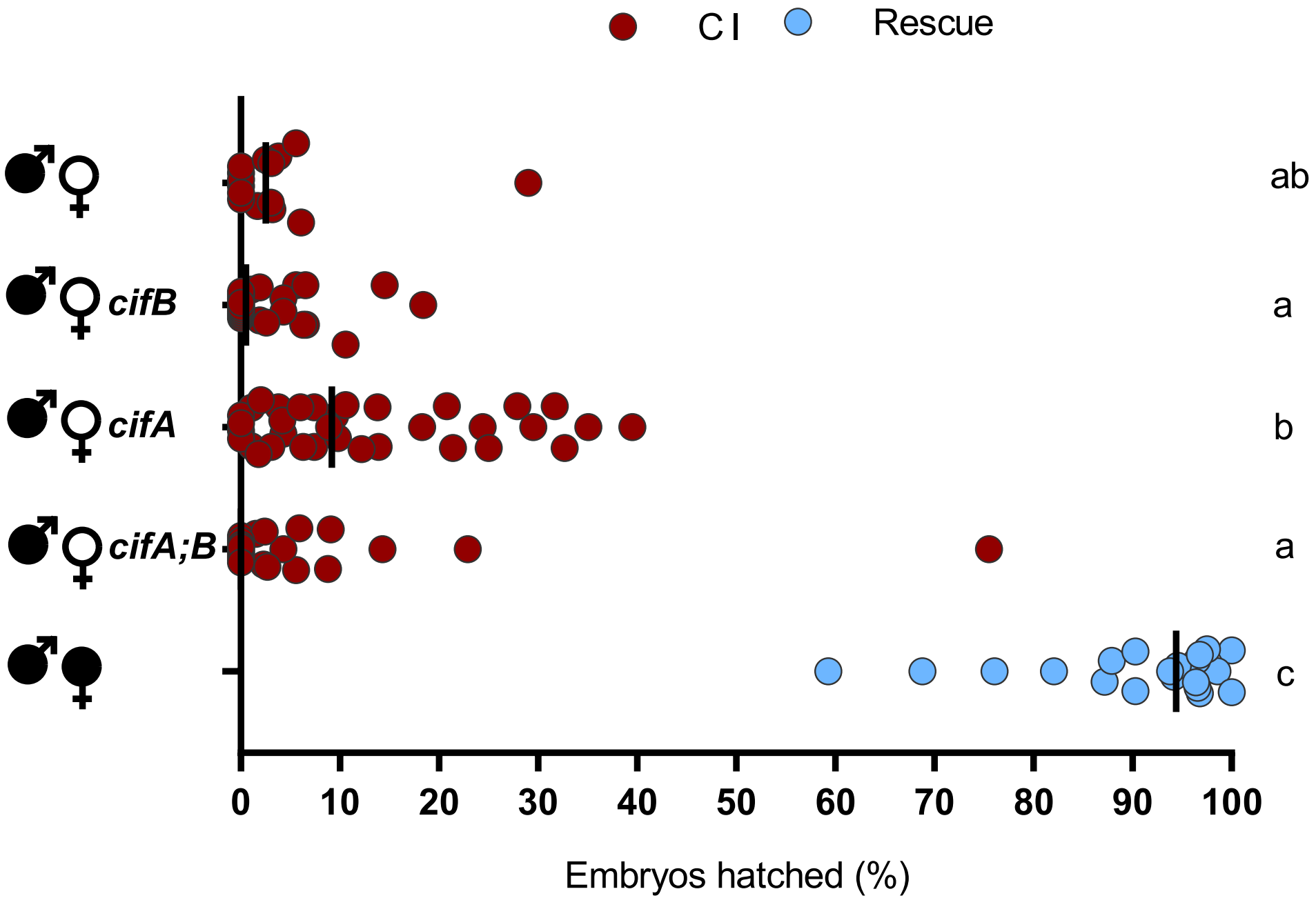
CI
Rescue
cifB
cifA
cifA;B
ab
a
b
a
c
0
10
20
30
40
50
60
70
80
90
100
Embryos hatched (%)

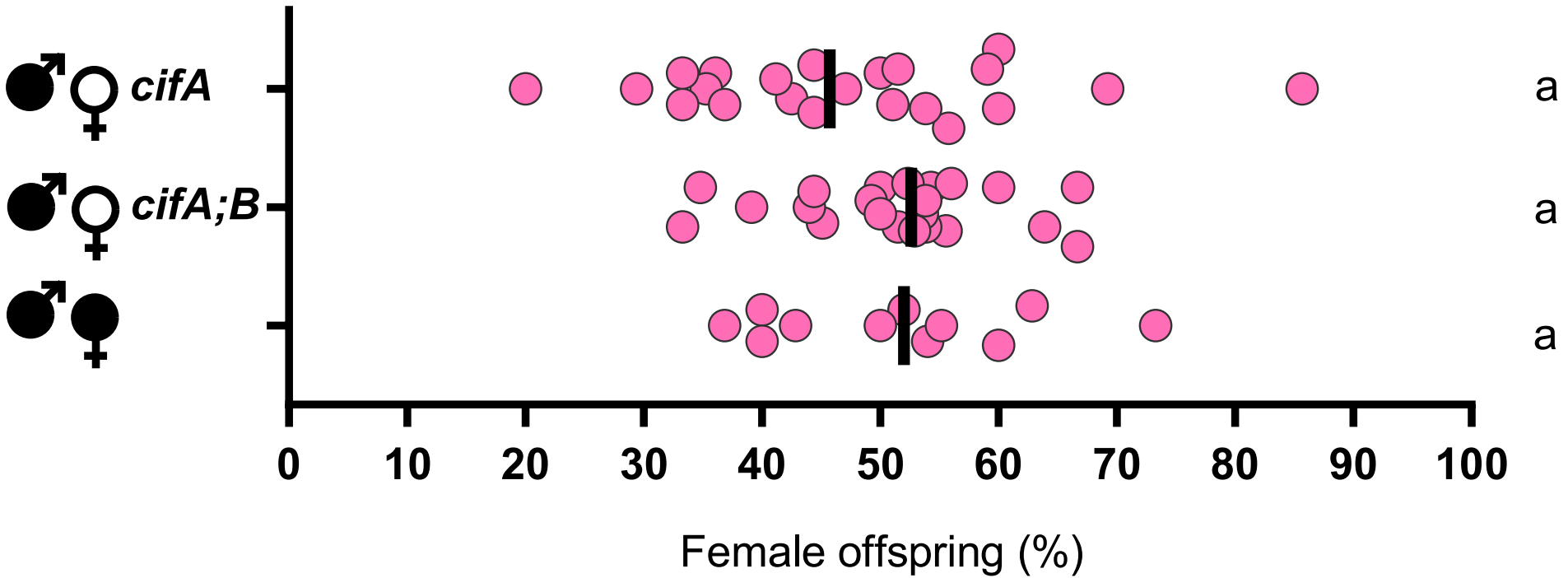
♂ ♀ cifA
♂ ♀ cifA;B
♂ ♀
a
a
a
0
10
20
30
40
50
60
70
80
90
100
Female offspring (%)

A PSORTb subcellular protein localization

	Accession	Cytoplasmic	Cytoplasmic Membrane	Periplasmic	Outer Membrane	Extracellular
wMel	WP_010962721.1	8.96	0.51	0.26	0.01	0.26
wRi	WP_012673191.1	8.96	0.51	0.26	0.01	0.26
wRec	WP_038198916.1	8.96	0.51	0.26	0.01	0.26
wSuzi	WP_044471237.1	8.96	0.51	0.26	0.01	0.26
wHa	WP_015588933.1	8.96	0.51	0.26	0.01	0.26
wSol	AGK87106.1	8.96	0.51	0.26	0.01	0.26
wBol 1-b	WP_019236549.1	8.96	0.51	0.26	0.01	0.26
wPip	WP_012481787.1	8.96	0.51	0.26	0.01	0.26

B

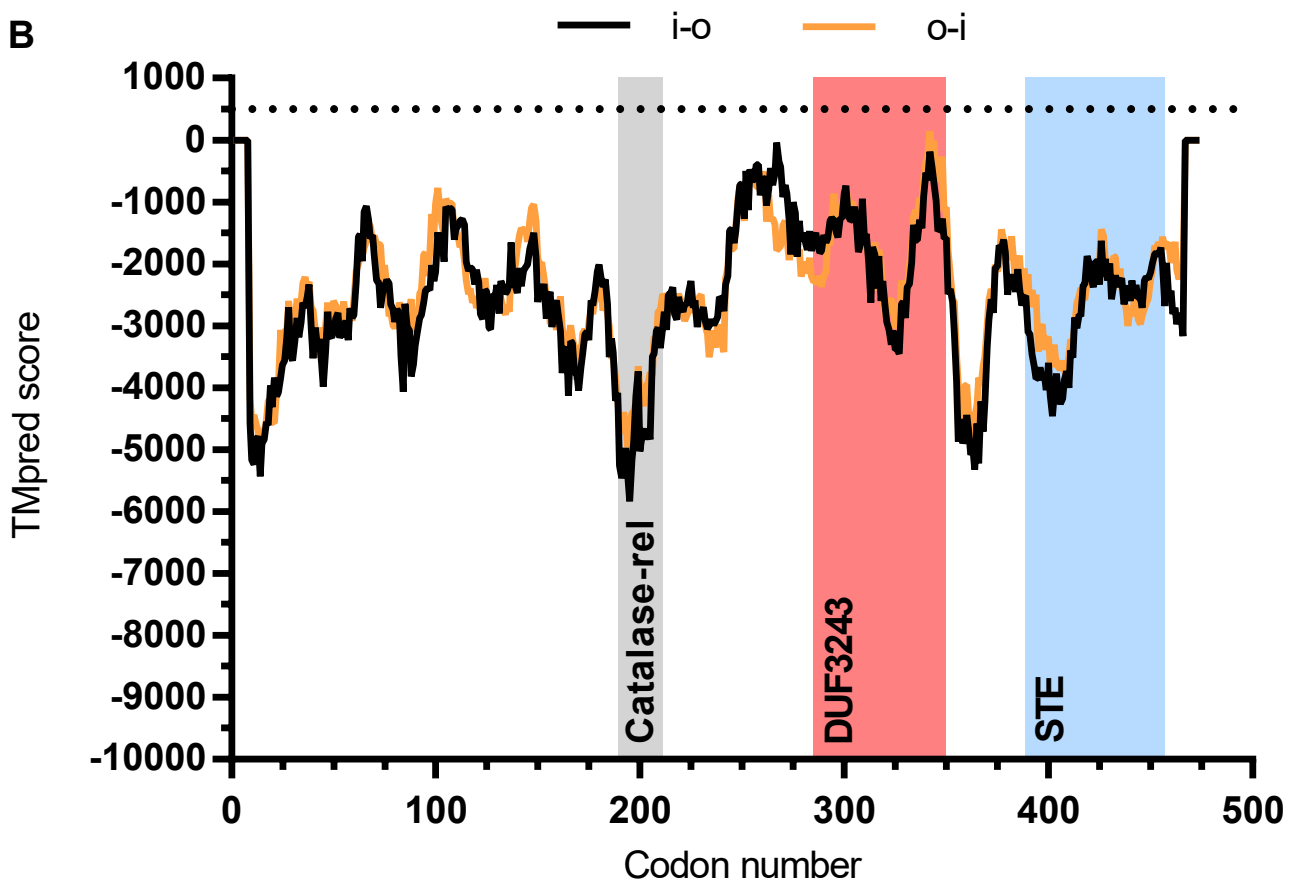

A Codon-based test of neutrality

	Accession	*w*Mel	*w*Ri	*w*Rec	*w*Suzi	*w*Ha	*w*Sol	*w*Bol 1-b	*w*Pip
***w*Mel**	NC_002978		2.241	-0.422	1.734	-7.316	-7.323	-6.388	-6.721
***w*Ri**	NC_012416	0.027		0.315	1.416	-7.355	-7.361	-6.426	-6.759
***w*Rec**	NZ_JQAM01000018	0.673	0.754		-0.161	-7.205	-7.211	-6.277	-6.609
***w*Suzi**	NZ_CAOU02000034	0.085	0.160	0.872		-7.412	-7.419	-6.484	-6.816
***w*Ha**	NC_021089	0.000	0.000	0.000	0.000		-1.206	-4.038	-3.929
***w*Sol**	KC955252	0.000	0.000	0.000	0.000	0.230		-4.229	-4.121
***w*Bol 1-b**	NZ_CAOH01000056	0.000	0.000	0.000	0.000	0.000	0.000		-1.603
***w*Pip**	NC_010981	0.000	0.000	0.000	0.000	0.000	0.000	0.112	

B Fisher's exact test of neutrality

	Accession	*w*Mel	*w*Ri	*w*Rec	*w*Suzi	*w*Ha	*w*Sol	*w*Bol 1-b	*w*Pip
***w*Mel**	NC_002978								
***w*Ri**	NC_012416	0.297							
***w*Rec**	NZ_JQAM01000018	1.000	0.618						
***w*Suzi**	NZ_CAOU02000034	0.483	0.616	1.000					
***w*Ha**	NC_021089	1.000	1.000	1.000	1.000				
***w*Sol**	KC955252	1.000	1.000	1.000	1.000	1.000			
***w*Bol 1-b**	NZ_CAOH01000056	1.000	1.000	1.000	1.000	1.000	1.000		
***w*Pip**	NC_010981	1.000	1.000	1.000	1.000	1.000	1.000	1.000	

C

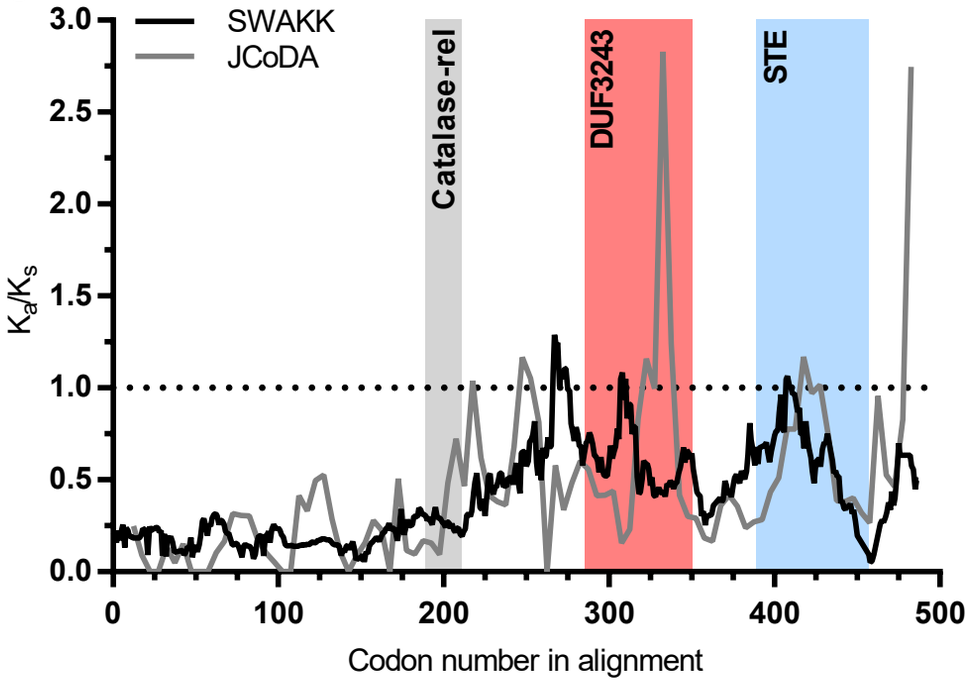

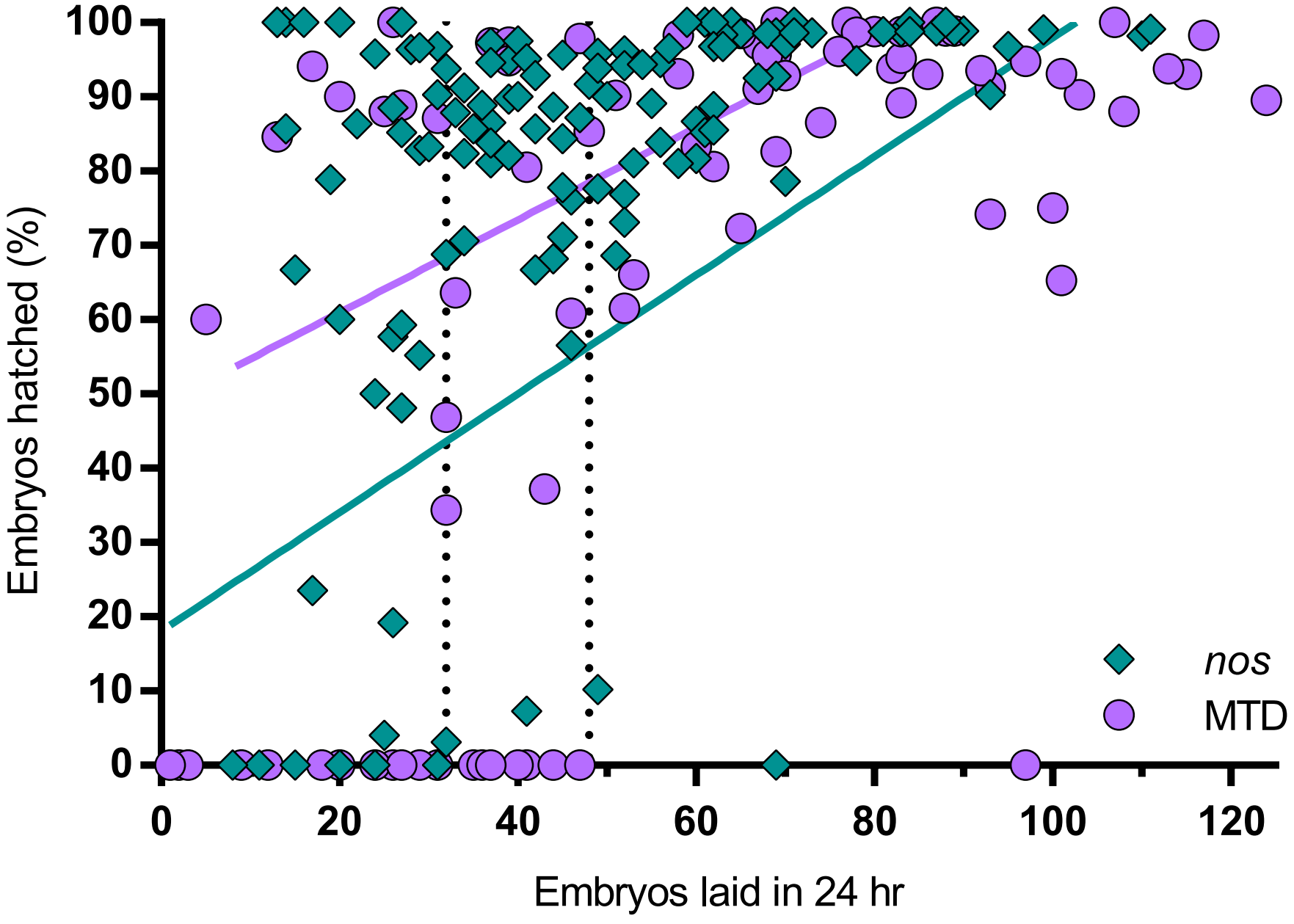
Embryos hatched (%)
100
90
80
70
60
50
40
30
20
10
0
0
20
40
60
80
100
120
Embryos laid in 24 hr
nos
MTD

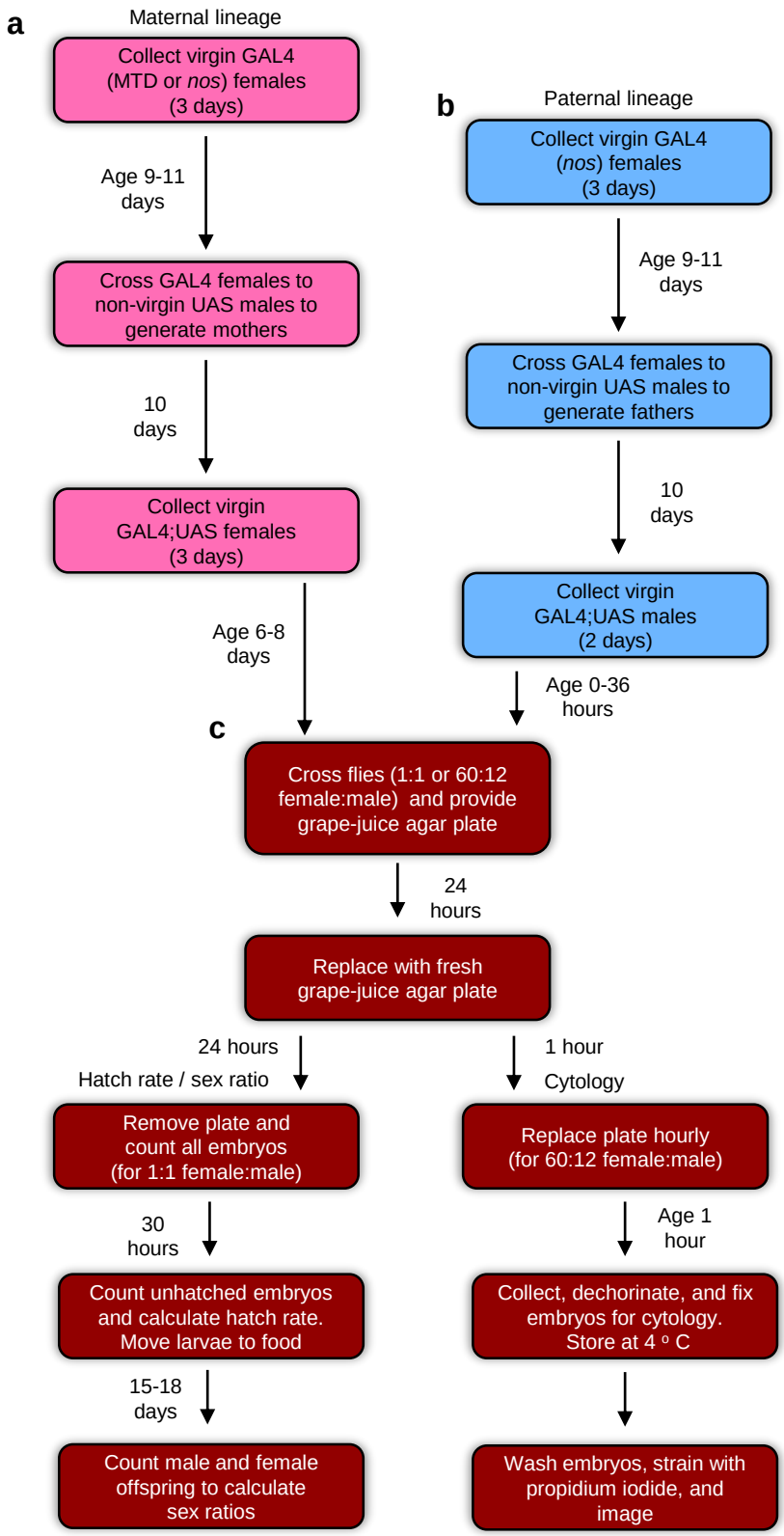
a
Maternal lineage
Collect virgin GAL4 (MTD or *nos*) females (3 days)
Age 9-11 days
Cross GAL4 females to non-virgin UAS males to generate mothers
10 days
Collect virgin GAL4;UAS females (3 days)
Age 6-8 days
b
Paternal lineage
Collect virgin GAL4 (*nos*) females (3 days)
Age 9-11 days
Cross GAL4 females to non-virgin UAS males to generate fathers
10 days
Collect virgin GAL4;UAS males (2 days)
Age 0-36 hours
c
Cross flies (1:1 or 60:12 female:male) and provide grape-juice agar plate
24 hours
Replace with fresh grape-juice agar plate
24 hours
Hatch rate / sex ratio
Remove plate and count all embryos (for 1:1 female:male)
30 hours
Count unhatched embryos and calculate hatch rate. Move larvae to food
15-18 days
Count male and female offspring to calculate sex ratios
1 hour
Cytology
Replace plate hourly (for 60:12 female:male)
Age 1 hour
Collect, dechorinate, and fix embryos for cytology. Store at 4 ° C
Wash embryos, strain with propidium iodide, and image

Table S1. Primers used in this study for RT-qPCR (Fig 1B) or for *Wolbachia* infection checks.

Primer	Sequence	Product Length (bp)
Rp49_F	CGGTTACGGATCGAACAAGC	154
Rp49_R	CTTGCGCTTCTTGGAGGAGA	
cifA opt_F	CCCGCTATTGCATCACAGGA	186
cifA opt_R	CGCGGTCGATCCAAAAATCG	
Wolb_F	GAAGATAATGACGGTACTCAC	990
Wolb_R3	GTCACTGATCCCACTTTAAATAAC	

F = forward primer, R = reverse primer.

Table S2. P-values associated with all statistical comparisons made in main and extended data figures.			
Figure	**Comparison**	**p-value**	**Test**
Fig. 1A	[M;+]nos;wt x [F;-]MTD;wt vs. [M;+]nos;wt x [F;-]MTD;cifA	**<0.0001**	Kruskal Wallis with Dunn's correction
	[M;+]nos;wt x [F;-]MTD;wt vs. [M;+]nos;wt x [F;+]MTD;wt	**<0.0001**	Kruskal Wallis with Dunn's correction
	[M;+]nos;wt x [F;-]MTD;wt vs. [M;+]nos;wt x [F;-]nos;wt	>0.9999	Kruskal Wallis with Dunn's correction
	[M;+]nos;wt x [F;-]MTD;wt vs. [M;+]nos;wt x [F;-]nos;cifA	>0.9999	Kruskal Wallis with Dunn's correction
	[M;+]nos;wt x [F;-]MTD;wt vs. [M;+]nos;wt x [F;+]nos;wt	**<0.0001**	Kruskal Wallis with Dunn's correction
	[M;+]nos;wt x [F;-]MTD;cifA vs. [M;+]nos;wt x [F;+]MTD;wt	>0.9999	Kruskal Wallis with Dunn's correction
	[M;+]nos;wt x [F;-]MTD;cifA vs. [M;+]nos;wt x [F;-]nos;wt	**<0.0001**	Kruskal Wallis with Dunn's correction
	[M;+]nos;wt x [F;-]MTD;cifA vs. [M;+]nos;wt x [F;-]nos;cifA	**<0.0001**	Kruskal Wallis with Dunn's correction
	[M;+]nos;wt x [F;-]MTD;cifA vs. [M;+]nos;wt x [F;+]nos;wt	>0.9999	Kruskal Wallis with Dunn's correction
	[M;+]nos;wt x [F;+]MTD;wt vs. [M;+]nos;wt x [F;-]nos;wt	**<0.0001**	Kruskal Wallis with Dunn's correction
	[M;+]nos;wt x [F;+]MTD;wt vs. [M;+]nos;wt x [F;-]nos;cifA	**<0.0001**	Kruskal Wallis with Dunn's correction
	[M;+]nos;wt x [F;+]MTD;wt vs. [M;+]nos;wt x [F;+]nos;wt	>0.9999	Kruskal Wallis with Dunn's correction
	[M;+]nos;wt x [F;-]nos;wt vs. [M;+]nos;wt x [F;-]nos;cifA	>0.9999	Kruskal Wallis with Dunn's correction
	[M;+]nos;wt x [F;-]nos;wt vs. [M;+]nos;wt x [F;+]nos;wt	**<0.0001**	Kruskal Wallis with Dunn's correction
	[M;+]nos;wt x [F;-]nos;cifA vs. [M;+]nos;wt x [F;+]nos;wt	**<0.0001**	Kruskal Wallis with Dunn's correction
Fig. 1B	nos-GAL4-tubulin vs. MTD-GAL4 cifA expression	**<0.0001**	Mann-Whitney test
Fig. 2	[M;+]nos;wt x [F;-]MTD;wt vs. [M;+]nos;wt x [F;-]MTD;cifA	**0.0379**	Kruskal Wallis with Dunn's correction
	[M;+]nos;wt x [F;-]MTD;wt vs. [M;+]nos;wt x [F;-]MTD;cifB	>0.9999	Kruskal Wallis with Dunn's correction
	[M;+]nos;wt x [F;-]MTD;wt vs. [M;+]nos;wt x [F;-]MTD;cifA;cifB	**0.0038**	Kruskal Wallis with Dunn's correction
	[M;+]nos;wt x [F;-]MTD;wt vs. [M;+]nos;wt x [F;+]MTD;wt	**0.0006**	Kruskal Wallis with Dunn's correction
	[M;+]nos;wt x [F;-]MTD;cifA vs. [M;+]nos;wt x [F;-]MTD;cifB	**0.0058**	Kruskal Wallis with Dunn's correction

	[M;+]nos;wt x [F;-]MTD;cifA vs. [M;+]nos;wt x [F;-]MTD;cifA;cifB	>0.9999	Kruskal Wallis with Dunn's correction
	[M;+]nos;wt x [F;-]MTD;cifA vs. [M;+]nos;wt x [F;+]MTD;wt	0.5436	Kruskal Wallis with Dunn's correction
	[M;+]nos;wt x [F;-]MTD;cifB vs. [M;+]nos;wt x [F;-]MTD;cifA;cifB	**0.0004**	Kruskal Wallis with Dunn's correction
	[M;+]nos;wt x [F;-]MTD;cifB vs. [M;+]nos;wt x [F;+]MTD;wt	**<0.0001**	Kruskal Wallis with Dunn's correction
	[M;+]nos;wt x [F;-]MTD;cifA;cifB vs. [M;+]nos;wt x [F;+]MTD;wt	>0.9999	Kruskal Wallis with Dunn's correction
Fig. 3	[M;+]nos;wt x [F;-]MTD;wt vs. [M;+]nos;wt x [F;-]MTD;cifA	**0.0010**	Chi-square with bonferroni adjusted p-value
	[M;+]nos;wt x [F;-]MTD;wt vs. [M;+]nos;wt x [F;-]MTD;cifB	0.4680	Chi-square with bonferroni adjusted p-value
	[M;+]nos;wt x [F;-]MTD;wt vs. [M;+]nos;wt x [F;-]MTD;cifA;cifB	**0.0010**	Chi-square with bonferroni adjusted p-value
	[M;+]nos;wt x [F;-]MTD;wt vs. [M;+]nos;wt x [F;+]MTD;wt	**0.0010**	Chi-square with bonferroni adjusted p-value
	[M;+]nos;wt x [F;-]MTD;cifA vs. [M;+]nos;wt x [F;-]MTD;cifB	**0.0010**	Chi-square with bonferroni adjusted p-value
	[M;+]nos;wt x [F;-]MTD;cifA vs. [M;+]nos;wt x [F;-]MTD;cifA;cifB	1.0000	Chi-square with bonferroni adjusted p-value
	[M;+]nos;wt x [F;-]MTD;cifA vs. [M;+]nos;wt x [F;+]MTD;wt	0.5740	Chi-square with bonferroni adjusted p-value
	[M;+]nos;wt x [F;-]MTD;cifB vs. [M;+]nos;wt x [F;-]MTD;cifA;cifB	**0.0010**	Chi-square with bonferroni adjusted p-value
	[M;+]nos;wt x [F;-]MTD;cifB vs. [M;+]nos;wt x [F;+]MTD;wt	**0.0010**	Chi-square with bonferroni adjusted p-value
	[M;+]nos;wt x [F;-]MTD;cifA;cifB vs. [M;+]nos;wt x [F;+]MTD;wt	**0.0030**	Chi-square with bonferroni adjusted p-value
Fig. S1	[M;+]nos;wt x [F;-]nos;wt vs. [M;+]nos;wt x [F;-]nos;cifA	0.1534	Kruskal Wallis with Dunn's correction
	[M;+]nos;wt x [F;-]nos;wt vs. [M;+]nos;wt x [F;-]nos;cifB	>0.9999	Kruskal Wallis with Dunn's correction
	[M;+]nos;wt x [F;-]nos;wt vs. [M;+]nos;wt x [F;-]nos;cifA;cifB	>0.9999	Kruskal Wallis with Dunn's correction
	[M;+]nos;wt x [F;-]nos;wt vs. [M;+]nos;wt x [F;+]nos;wt	**<0.0001**	Kruskal Wallis with Dunn's correction
	[M;+]nos;wt x [F;-]nos;cifA vs. [M;+]nos;wt x [F;-]nos;cifB	**0.0204**	Kruskal Wallis with Dunn's correction
	[M;+]nos;wt x [F;-]nos;cifA vs. [M;+]nos;wt x [F;-]nos;cifA;cifB	**0.0306**	Kruskal Wallis with Dunn's correction
	[M;+]nos;wt x [F;-]nos;cifA vs. [M;+]nos;wt x [F;+]nos;wt	**0.0001**	Kruskal Wallis with Dunn's correction
	[M;+]nos;wt x [F;-]nos;cifB vs. [M;+]nos;wt x [F;-]nos;cifA;cifB	>0.9999	Kruskal Wallis with Dunn's correction

	[M;+]nos;wt x [F;-]nos;cifB vs. [M;+]nos;wt x [F;+]nos;wt	**<0.0001**	Kruskal Wallis with Dunn's correction
	[M;+]nos;wt x [F;-]nos;cifA;cifB vs. [M;+]nos;wt x [F;+]nos;wt	**<0.0001**	Kruskal Wallis with Dunn's correction
Fig. S2	[M;+]nos;wt x [F;-]MTD;cifA vs. [M;+]nos;wt x [F;-]MTD;cifA;cifB	0.5209	Kruskal Wallis with Dunn's correction
	[M;+]nos;wt x [F;-]MTD;cifA vs. [M;+]nos;wt x [F;+]MTD;wt	0.8609	Kruskal Wallis with Dunn's correction
	[M;+]nos;wt x [F;-]MTD;cifA;cifB vs. [M;+]nos;wt x [F;+]MTD;wt	>0.9999	Kruskal Wallis with Dunn's correction
Fig. S5	Hatch rate vs clutch size (MTD-GAL4)	**<0.0001**	Spearman's Rho
	Hatch rate vs clutch size (nos-GAL4-tubulin)	**<0.0001**	Spearman's Rho
M = male, F = female, + = *Wolbachia* infected, - = *Wolbachia* uninfected, bold p-values = significant			